A multi-sensor array for detecting and analyzing nocturnal avian migration

Alva I Strand [Corresp., 1, 2] , **Eli S Bridge** [2] , **Jeffrey F Kelly** [1, 2] , **Phillip M Stepanian** [3] , **David J Bodine** [4, 5] , **James R Soto** [2]

[1] Department of Biology, University of Oklahoma, Norman, Oklahoma, United States

[2] Oklahoma Biological Survey, University of Oklahoma, Norman, Oklahoma, United States

[3] Department of Civil and Environmental Engineering and Earth Sciences, University of Notre Dame, Notre Dame, Indiana, United States

[4] Advanced Radar Research Center, University of Oklahoma, Norman, Oklahoma, United States

[5] School of Meteorology, University of Oklahoma, Norman, Oklahoma, United States

Corresponding Author: Alva I Strand
Email address: alvastrand@ou.edu

Avian migration has fascinated humans for centuries. Insights into the lives of migrant birds are often elusive; however, recent, standalone technological innovations have revolutionized our understanding of this complex biological phenomenon. A future challenge for following these highly mobile animals is the necessity of bringing multiple technologies together to capture a more complete understanding of their movements. Here, we designed a proof-of-concept multi-sensor array consisting of two weather surveillance radars (WSRs), one local and one regional, an autonomous moon-watching sensor capable of detecting birds flying in front of the moon, and an autonomous recording unit (ARU) capable of recording avian nocturnal flight calls. We deployed this array at a field site in central Oklahoma on select nights in March, April, and May of 2021 and integrated data from this array with wind data corresponding to this site to examine the influence of wind on the movements of spring migrants aloft across these spring nights. We found that regional avian migration intensity is statistically significantly negatively correlated with wind velocity, in line with previous research. Furthermore, we found evidence suggesting that when faced with strong, southerly winds, migrants take advantage of these conditions by adjusting their flight direction by drifting. Importantly, we found that most of the migration intensities detected by the sensors were intercorrelated, except when this correlation could not be ascertained because we lacked the sample size to do so. This study demonstrates the potential for multi-sensor arrays to reveal the detailed ways in which avian migrants move in response to changing atmospheric conditions while in flight.

1 A multi-sensor array for detecting and analyzing nocturnal avian migration

3 Alva I. Strand[1,2], Eli S. Bridge[2], Jeffrey F. Kelly[1,2], Phillip M. Stepanian[3], David J. Bodine[4,5],
4 James R. Soto[2]
5
6 [1] Department of Biology, University of Oklahoma, Norman, OK, USA
7 [2] Oklahoma Biological Survey, University of Oklahoma, Norman, OK, USA
8 [3] Department of Civil and Environmental Engineering and Earth Sciences, University of Notre
9 Dame, Notre Dame, IN, USA
10 [4] School of Meteorology, University of Oklahoma, Norman, OK, USA
11 [5] Advanced Radar Research Center, University of Oklahoma, Norman, OK, USA
12
13 Corresponding Author:
14 Alva I. Strand[1,2]
15 111 Chesapeake St., Norman, OK 73019, USA
16 Email address: alvastrand@ou.edu

18 Abstract

20 Avian migration has fascinated humans for centuries. Insights into the lives of migrant birds are
21 often elusive; however, recent, standalone technological innovations have revolutionized our
22 understanding of this complex biological phenomenon. A future challenge for following these
23 highly mobile animals is the necessity of bringing multiple technologies together to capture a
24 more complete understanding of their movements. Here, we designed a proof-of-concept multi-
25 sensor array consisting of two weather surveillance radars (WSRs), one local and one regional,
26 an autonomous moon-watching sensor capable of detecting birds flying in front of the moon,
27 and an autonomous recording unit (ARU) capable of recording avian nocturnal flight calls. We
28 deployed this array at a field site in central Oklahoma on select nights in March, April, and May
29 of 2021 and integrated data from this array with wind data corresponding to this site to examine
30 the influence of wind on the movements of spring migrants aloft across these spring nights. We
31 found that regional avian migration intensity is statistically significantly negatively correlated with
32 wind velocity, in line with previous research. Furthermore, we found evidence suggesting that
33 when faced with strong, southerly winds, migrants take advantage of these conditions by
34 adjusting their flight direction by drifting. Importantly, we found that most of the migration
35 intensities detected by the sensors were intercorrelated, except when this correlation could not
36 be ascertained because we lacked the sample size to do so. This study demonstrates the
37 potential for multi-sensor arrays to reveal the detailed ways in which avian migrants move in
38 response to changing atmospheric conditions while in flight.

39
40 Introduction
41
42   Every spring and fall, billions of birds migrate, and yet, despite this enormous number,
43 large gaps remain in our understanding of avian migration. In fact, avian migration is challenging
44 to study because migratory birds are small and move across vast spatial and temporal scales,

45 often at night. To this end, several remote-sensing technologies have emerged to study the
46 movements of avian migrants (Bridge et al., 2011; McKinnon & Love, 2018; Robinson et al.,
47 2010). One such technology that has been successfully used to unravel the complexities of
48 avian migration is weather surveillance radar (WSR), particularly in the United States, as the
49 spatial and temporal coverage of the U.S. network of WSRs, called NEXt-Generation Weather
50 RADar (NEXRAD, or WSR-88D), is extensive. Additionally, NEXRAD collects data nearly
51 continuously, and these data are openly accessible. Indeed, WSRs have been used to monitor
52 animal activity (Kelly et al., 2017; Kelly & Horton, 2016), extrapolate population estimates (Clark
53 et al., 2020), and identify trends that correlate with land use and climate change (Bridge et al.,
54 2016). However, this technology suffers from three major shortcomings. Firstly, in most cases,
55 WSRs cannot be used to identify species aloft. Secondly, although WSRs have been used to
56 estimate mean flight directions and velocities of migrants (Horton et al., 2016), they cannot
57 detect individual flight characteristics, including individual flight directions, flight velocities, and
58 body orientations. Thirdly, NEXRAD WSRs have a range bias that makes it challenging to
59 detect low-flying birds (Buler & Diehl, 2009; Diehl & Larkin, 2005). Therefore, integrating
60 NEXRAD WSR data with data from other remote sensors that can address these limitations
61 would enhance our ability to study avian migrants.
62   To demonstrate the utility of doing so, we designed a proof-of-concept multi-sensor
63 array. This array consisted of two WSRs (the KTLX WSR from the NEXRAD network and a
64 portable, dual-polarization X-band WSR called PX-1000 (Cheong et al., 2013)), a novel,
65 automated observational sensor based on traditional moon-watching called LunAero (Honeycutt
66 et al., 2020; Honeycutt & Bridge, 2022), and a microphone capable of recording avian nocturnal
67 flight calls. We deployed this array at the University of Oklahoma Kessler Atmospheric and
68 Ecological Field Station (KAEFS) on select nights in March, April, and May of 2021. Data from
69 this array were then integrated with wind data from the National Centers for Environmental
70 Prediction (NCEP)'s North American Regional Reanalysis (NARR) to investigate the influence of
71 this abiotic variable on avian migrants in flight. We chose to include a microphone, a moon-
72 watching sensor, and a portable WSR in our array because each of these sensors addressed
73 one of the three limitations of NEXRAD WSRs described above. The microphone, coupled with
74 knowledge of avian species' nocturnal flight calls, allows us to identify species migrating aloft.
75 LunAero, the moon-watching sensor, can be used to derive flight directions of individual birds
76 and provide insights into wind-drift compensation of individual migrants (Honeycutt et al., 2020;
77 Honeycutt & Bridge, 2022). Finally, PX-1000, the portable WSR, can be used to detect local
78 migrants flying at low altitudes (Cheong et al., 2013).
79   With this multi-sensor array, we sought to answer two major questions:
80   1. Are the avian migration intensities detected by all of the sensors intercorrelated?
81   2. Could integration of sensor data enable inferences about the influence of wind on avian
82   migration?
83   Firstly, we needed to validate the ability of LunAero and PX-1000 to detect birds, as
84 these are novel sensors. We predicted that the number of individual birds detected by LunAero
85 would be positively correlated with the regional intensity of avian migration from the KTLX radar.
86 We also predicted that the local intensity of avian migration detected by PX-1000 would be
87 positively correlated with the regional avian migration intensity detected by the KTLX radar.

88   Secondly, we wanted to investigate whether we could use data from the multi-sensor
89 array that we designed and integrate it with wind data from NARR to demonstrate how such a
90 multi-sensor array could be used to study how birds respond to changing wind conditions during
91 spring migration. To do so, we set out to verify that the wind directions and velocities from
92 NARR on the nights in question matched our expectations. We predicted that most winds,
93 including the fastest ones, would be southerly (blowing from south to north), as the Great Plains
94 low-level jet (LLJ) provides strong, southerly winds across our study site in the spring
95 (Wainwright et al., 2016). Next, we wanted to use data from the KTLX radar and NARR to
96 identify the wind conditions favored by migrants across select nights in the spring. We predicted
97 that they would favor southerly (tail) winds, as birds migrate from south to north in the spring, in
98 addition to weaker winds.
99   Importantly, we wanted to leverage data on individual migrants from LunAero and
100 integrate it with data from NARR to determine the ways in which wind conditions influence the
101 flight directions of individual migrants in the spring. We predicted that when exposed to stronger
102 southerly winds, migrants would adjust their flight directions to drift. That is, as the velocity of
103 the wind increases, we predicted that the difference between the direction of the wind and the
104 flight direction of an individual migrant would decrease. We made this prediction for southerly
105 winds, as the direction of those winds is the same as that in which birds migrate in the spring.
106 Finally, we wanted to investigate whether we could integrate avian nocturnal flight call data with
107 data from other sensors to examine whether different avian species favor different wind
108 conditions during migration.
109
110 Materials & Methods
111
112 Study Site
113
114   All observations were made from March to May of 2021 in the lower atmosphere above
115 the University of Oklahoma Kessler Atmospheric and Ecological Field Station (KAEFS) (34.98°
116 N, 97.52° W). KAEFS encompasses ~146 ha at ~350 meters above mean sea level and
117 features large patches of mixed-grass prairie that provide a full view of the sky.
118
119 Temporal Sampling
120
121   The instruments deployed at KAEFS included an automated moon-watching apparatus,
122 the PX-1000 x-band radar, and an autonomous recording unit (ARU) to record audio data. The
123 moon-watching equipment was deployed only within five days of a full moon, and the data were
124 only usable when the sky was clear of clouds. The ARU was deployed throughout the period
125 surrounding the full moon, and the PX-1000 collected data continuously for the entire spring.
126 However, the data used in this paper is restricted to six nights for which we had moon-watching
127 footage. These nights were March 26, March 27, March 28, March 29, April 24, and May 25,
128 2021. Furthermore, because the ARU did not detect any migrant species on the nights of March
129 26 and March 28, only ARU data for four nights (the nights of March 27, March 29, April 24, and
130 May 25) could be and were analyzed.
131

132 NEXRAD Weather Surveillance Radar (WSR) Data

133

134   KAEFS is located ~45 km southwest of the nearest NEXRAD weather surveillance radar
135 (WSR), which is the KTLX radar (35.34° N, 97.28° W). To estimate regional intensity of avian
136 migration, data from KTLX were accessed from the Amazon Web Service radar archive
137 (https://registry.opendata.aws/noaa-nexrad/). We opened each radar file using PyART (Helmus
138 & Collis, 2016), censored weather by removing pixels with a depolarization ratio less than -12.5
139 dB (Kilambi et al., 2018), limited the analysis range to within 60 km of the radar, and manually
140 removed clutter from a wind farm west of the radar site. To create vertical profiles of reflectivity
141 (VPRs), we determined the altitude of each remaining radar gate center and assigned the
142 corresponding reflectivity (in cm2/km3) to this altitude. Reflectivities were averaged within 100-
143 meter altitudinal bins (starting at 0 meters above mean sea level), yielding a single reflectivity
144 value per bin. Reflectivities between 400 and 1,300 meters above mean sea level (between ~50
145 and ~950 meters above ground level) were summed and multiplied by 0.1 kilometer to account
146 for altitudinal bin height, yielding a single reflectivity value per VPR in cm2/km2 (Chilson, Frick,
147 Kelly, et al., 2012; Chilson, Frick, Stepanian, et al., 2012). Reflectivities for each VPR were then
148 summed for each one-hour period, yielding a single summed reflectivity value for each
149 combination of date and hour, hereafter referred to as the regional intensity of avian migration
150 from the KTLX radar for each combination of date and hour.

151

152 Wind Data

153

154   To examine the influence of wind on nocturnal avian migration, we made use of wind
155 data from the National Centers for Environmental Prediction (NCEP)'s North American Regional
156 Reanalysis (NARR) data set. This data set provides weather data based on an interpolation
157 model for 32 km grid cells that encompass North America. NARR data have a temporal
158 resolution of 3 hours. We downloaded wind data from the NCEP's Global Reanalysis page
159 (https://psl.noaa.gov/data/gridded/data.narr.html) and extracted wind velocity (in meters per
160 second) and direction (in degrees clockwise from north) from the grid cell overlapping KAEFS
161 (35.18° N, 97.44° W). Each wind profile was integrated across altitudes by calculating the mean
162 wind velocity and direction between 400 and 1,300 meters above sea level.

163

164 Moon-watching (LunAero) Data

165

166   Moon-watching is a method of quantifying nocturnal bird migration, wherein one uses the
167 moon as an illumination source to count the silhouettes of birds that fly between the moon and
168 the observer. Although moonwatching has been employed by researchers on several continents
169 (Hilgerloh et al., 2006; Liechti et al., 1995; Lowery, 1949; Lowery & Newman, 1966; Nisbet,
170 1959; Trösch et al., 2005; Weisshaupt et al., 2016; Zehtindjiev & Liechti, 2003), more
171 widespread use has been limited by challenges relating to accuracy of the method and the
172 observational rigor required when collecting data manually in real time. We used the LunAero
173 automated moon-watching sensor to observe bird migration by making video recordings of the
174 moon and identifying bird flight paths using computer vision software (Honeycutt et al., 2020;
175 Honeycutt & Bridge, 2022).

176   The analysis workflow for extracting migratory bird information from videos is summarized
177 below. All analyses were done in the R programming environment (R Core Team, 2022) and
178 used Stellarium, an open-source planetarium (Zotti et al., 2021). Briefly, the analysis pathway
179 was as follows:
180
181   1. We used computer vision tools available in Rvision (Garnier & Muschelli, 2022), which is
182   a wrapper for OpenCV (Bradski, 2000) to identify dark pixel clusters (henceforth
183   contours) in each frame of video using the dynamic thresholding function. The contours
184   identified by this process included both bird silhouettes and a considerable amount of
185   noise associated with camera movement and dark features on the moon. We applied
186   some filtering based on co-occurrence across frames to remove contours that were likely
187   to be due to moon craters, and we ranked contours according to how distinct they were
188   from the immediate background (more distinct contours were more likely to be actual
189   bird silhouettes).
190   2. The next analysis step examined all of the extracted contours and attempted to
191   assemble them into linear series of points across a series of video frames. Each contour
192   not already assigned to a track was compared with all contours from three previous and
193   three subsequent frames to find potential flight paths. If a series of at least three
194   contours was detected that met a threshold for linearity, the search for contours was
195   extended to add to the potential flight path. Any contours added to a flight path were
196   flagged such that they could not contribute to another flight path. The results of this step
197   generally yielded a majority of real flight paths, but instances where paths were
198   assembled from false contours were frequent. These false detections were usually
199   evident when filtering examining by the linearity of the contours, the number of contours
200   comprising a path, and the distinctiveness of the contours.
201   3. To remove false paths, we visually inspected sets of video frames associated with paths
202   that were questionable as indicated by low contour counts, reduced linearity, and very
203   faint contours. We also visually inspected distinct contours that were not linked to be a
204   flight path to ensure that we did not fail to detect any birds.
205   4. When collecting video footage, we did not ensure that the recorded images were aligned
206   with true horizontal, which would affect assignment of flight directions. To correct for
207   potentially rotated video footage, we aligned moon images from our video with vertically
208   aligned images from the Stellarium software package (Zotti et al., 2021). The rotation
209   factor required for this alignment was used to adjust the x and y coordinates of the flight
210   paths to correct for the misalignment of the camera with the horizontal plane.
211   5. We transformed the x and y coordinates to situate them on a horizontal plane parallel to
212   the earth's surface and we rotated them such that the direction of each flight path could
213   be measured in degrees east of north.
214
215 PX-1000 Weather Surveillance Radar (WSR) Data
216
217   The PX-1000 radar was collocated with the moonwatching equipment at KAEFS. The
218 PX-1000 is a transportable, solid-state, polarimetric radar with independent horizontal and
219 vertical polarizations. The radar scanned at a frequency of 9550 MHz at elevation angles of 4 to

220   10 degrees at 2-degree increments, while rotating 360 degrees every 20 seconds. The PX-1000
221   recorded data continuously throughout each night of data collection. However, we used different
222   radar pulse settings in May compared to March and April. In March and April, we used a pulse
223   duration of 67-microseconds, which is typical for use in scanning long range targets (e.g.,
224   objects more than 5 km away). Using pulse compression, range resolution of 30 meters is
225   obtained with these settings (Kurdzo et al., 2014). The longer pulse lengths involve emission of
226   more radar energy on average, which makes the radar sensitive to more distant scatterers, but
227   it limits the extent to which we can resolve reflectivity from objects that are close to the radar
228   (e.g., within 10 km). In May, a new pulse compression technique was used that involves
229   simultaneous transmission and reception and increases sensitivity at close range by ~10 dB
230   (Aquino et al., 2021). Mirroring our method of processing the KTLX radar data, we obtained
231   summed reflectivity values for each 10-minute time period, hereafter referred to as local
232   intensity of avian migration from the PX-1000 radar for each combination of date and time
233   period.
234
235   Nocturnal Flight Call Recorder and Detection
236
237   We recorded nocturnal flight calls with a pressure zone microphone (Wildtronics Micro
238   Mic PIP Microphone, Newton Falls, Ohio, USA) attached to an Audiomoth Autonomous
239   Recording Unit (ARU) (Hill et al., 2019). The microphone and support apparatus were
240   constructed following the OldBird 21 c Pressure Zone Microphone design developed by Bill
241   Evans (http://www.oldbird.org/mic/21c.htm). The microphone was positioned at the apex of an
242   inverted plexiglass pyramid designed to increase the gain of audio recordings. The pyramid was
243   supported by a plexiglass pedestal that rested inside a plastic 2-gallon bucket with the
244   microphone pointing upward to the sky. The bucket served to minimize background sounds
245   (e.g., insects) from below. Plastic wrap was taped in place over the pyramid and pedestal to
246   provide a waterproof cover for the microphone. The Audiomoth was placed in a waterproof
247   container attached to the bottom of the bucket with the microphone cord inserted through it.
248   We recorded avian nocturnal flight calls from March 25, 2021 to May 31, 2021; however, we
249   restricted our analysis of the ARU data to six nights in March, April, and May for which there
250   was LunAero data (see Temporal Sampling). Furthermore, because the ARU did not detect any
251   migrant species on the nights of March 26 and March 28, only ARU data for four nights (March
252   27, March 29, April 24, and May 25) could be and were analyzed. Each day, recording started at
253   2000 Central Time (0100 UTC) and ended at 0700 Central Time (1200 UTC). We analyzed
254   Audio Recordings with the Vesper Audio Analysis Program (© Copyright 2020, Harold Mills
255   Revision aa3ad038) which processes the audio recordings then generates spectrograms of brief
256   audio segments that the program identifies as potential flight calls. Vesper generates these
257   audio segments or "clips" using multiple detectors that scan the entire audio for specified
258   frequencies and amplitudes.
259   We examined all of the clips generated by Vesper analysis and assigned them to
260   species by visually comparing clip spectrograms to reference spectrograms generated from
261   Flight Calls of Migratory Birds (Evans & O'Brien, 2002), Rosetta Stone to the Warblers
262   (Farnsworth, 2011), studies of various call complexes (Landsborough et al., 2019), and personal
263   recordings of known species observed in the field. We used Raven Pro Software Version 1.6.3

264   (K. Lisa Yang Center for Conservation Bioacoustics at the Cornell Lab of Ornithology, 2022) to
265   measure length of calls, determine specific frequencies of calls, measure distance between
266   modulation peaks of certain calls, and listen to calls and the entirety of the audio recordings
267   when needed. We compiled data for all species detected and all flight calls. We then filtered out
268   all non-migratory species and resolved all calls that were likely repeated vocalizations from the
269   same individual into a single detection based on the timing and relative volume of the recorded
270   vocalization.
271
272   Statistical analysis
273
274   To validate the ability of the LunAero moon-watching sensor to detect birds, we
275   compared the number of individual birds detected by LunAero with the regional intensity of
276   avian migration from the KTLX radar for each of six nights in March, April, and May of 2021 and
277   each hour for which there was data. That is, we calculated both the number of individual birds
278   detected and the regional migration intensity for each combination of date and hour, matched
279   these numbers with one another based on the date and hour, and calculated Pearson's
280   correlation coefficient as a measure of the strength and direction of the correlation between
281   these two variables across these nights.
282   To validate the ability of the PX-1000 radar to detect birds, we compared the local
283   intensity of avian migration from PX-1000 with the regional intensity of avian migration from the
284   KTLX radar by matching each migration intensity value of KTLX (for a ~10-minute time period
285   and one of the six nights in March, April, and May of 2021) to the migration intensity value of
286   PX-1000 closest in time to it (also calculated for a 10-minute time period). Then, we calculated
287   Pearson's correlation coefficient as a measure of the strength and direction of the correlation
288   between these two variables across nights.
289   To showcase how this multi-sensor array could be used to study the influence of wind on
290   avian migration, we compared regional migration intensity data from KTLX and wind data from
291   NARR by matching each migration intensity value of KTLX (for a ~10-minute time period and
292   one of the six nights in March, April, and May of 2021) to the wind velocity value closest in time
293   to the migration intensity value. Then, we calculated Pearson's correlation coefficient as a
294   measure of the strength and direction of the correlation between these two variables across
295   nights.
296   Finally, to demonstrate the utility of LunAero as a tool to study the individual movements
297   of birds during migration, we compared flight directions of individual migrants detected by
298   LunAero with those of winds from NARR by, once again, matching each individual bird detection
299   by LunAero with the wind velocity and direction values closest in time to it. Finally, we calculated
300   Pearson's correlation coefficient as a measure of the strength and direction of the correlation
301   between these two variables across nights.
302
303   Results
304
305   To validate the ability of the LunAero moon-watching sensor to detect birds, we
306   compared the number of individual birds detected by LunAero with the regional intensity of
307   avian migration from the KTLX radar. We found that these two variables are positively and

308   statistically significantly correlated with each other on five nights in March and April of 2021
309   (r(31) = 0.714, *p* < .001), although the strength of this correlation decreases and the correlation
310   ceases to be statistically significant with the inclusion of data collected on the night of May 25,
311   2021 (between 10 PM and 1 AM) (r(34) = 0.322, *p* = .0553) (Figure 1).
312   To validate the ability of PX-1000 to detect birds, we compared the local intensity of
313   avian migration from PX-1000 with the regional intensity of avian migration from the KTLX radar.
314   We found that the strength of the positive correlation between these two measures of migration
315   intensity hinges on the way in which the PX-1000 radar data is processed. In May, the way in
316   which the PX-1000 data was processed was modified to increase sensitivity at close range.
317   Consequently, we found that the correlation between the local migration intensity from PX-1000
318   and the regional migration intensity from the KTLX radar is strong and statistically significant for
319   the night of May 25, 2021 (r(168) = 0.768, *p* < .001; Figure 2A) but weak and not statistically
320   significant across five nights in March and April (r(320) = -0.0977, *p* = .0799; Figure 2B).
321   Next, we analyzed wind data from NARR to confirm that the wind conditions on the
322   nights of March 26, March 27, March 28, March 29, April 24, and May 25, 2021 matched our
323   expectations. We found that most of the winds were southerly (blowing from south to north), as
324   expected (Figure 3). Furthermore, we found that the fastest winds were southerly, as expected
325   (Figure 3).
326   We also used regional avian migration intensity data from the KTLX radar and wind data
327   from NARR corresponding to these dates in the spring of 2021 to determine the wind conditions
328   favored by migrant birds across these dates, demonstrating the use of this multi-sensor array as
329   a tool to study avian migration. We found a statistically significant, negative correlation between
330   regional migration intensity and wind velocity, suggesting that migrant birds favor weaker winds
331   (r(490) = -0.259, *p* < .001; Figure 4).
332   We also compared the flight directions of individual migrant birds detected by LunAero
333   with those of winds from NARR to understand the ways in which migrant birds respond to
334   changing wind conditions across these dates. For southerly winds, we found that as the velocity
335   of the wind increases, the difference between the direction of the wind and the flight direction of
336   the individual migrant decreases and that this negative correlation is statistically significant
337   (r(1153) = -0.284, *p* < .001; Figure 5A). We did not find a statistically significant correlation
338   between wind velocity and the difference between wind and flight directions for northerly winds
339   (r(868) = 0.0686, *p* = .0415; Figure 5B).
340   Finally, we used nocturnal flight call recordings to analyze the avian migrant species
341   composition of the lower atmosphere above the University of Oklahoma Kessler Atmospheric
342   and Ecological Field Station (KAEFS) on four nights in March, April, and May of 2021. We
343   recorded the largest number of individual migrants on the night of April 24 (41 individual birds
344   and 11 species) and the second-largest number of individual migrants on the night of May 25
345   (19 individual birds and 3 species) (Table 1). Notably, we recorded 14 Upland Sandpipers on
346   the night of April 24 and 17 Swainson's Thrushes on the night of May 25 (Table 1). Due to the
347   small sample size of the nocturnal flight call data, we could not make inferences about the
348   relationship between the number of migrants recorded and the number of migrants detected by
349   LunAero and the relationship between nocturnal flight calls and wind conditions during
350   migration.
351

352   Discussion
353
354   The challenges of studying avian migration have spurred the development of a number
355   of remote-sensing technologies to detect migrant birds. As each of these technologies have
356   their strengths and weaknesses, efforts have been made to use them in tandem; however, a
357   majority of these efforts have been limited to two technologies ((Gauthreaux & Belser, 1998;
358   Larkin et al., 2002; Weisshaupt et al., 2021) or to radar technologies only (Liechti et al., 2019;
359   Nilsson et al., 2018), although researchers have increasingly been exploring the utility of
360   combining more than two different types of technologies (Liechti et al., 1995; Weisshaupt et al.,
361   2017)). We designed a proof-of-concept multi-sensor array, integrating data from multiple
362   technologies to detect migrants in flight and elucidate the ways in which birds respond to
363   changing wind conditions during spring migration.
364   We found a strong, statistically significant, positive correlation between the number of
365   birds detected by LunAero and the regional intensity of avian migration detected by the KTLX
366   radar on five nights in March and April of 2021, validating the ability of LunAero to detect birds
367   (Figure 1). However, this correlation decreased and ceased to be statistically significant with the
368   inclusion of data collected on the night of May 25, 2021 (Figure 1). It is unclear why the
369   relationship between these two variables differed on this night. While it is possible that LunAero
370   is unable to detect birds flying above a certain altitude, we performed an analysis that suggests
371   that migrant altitude does not explain why LunAero did not detect many birds on that night. In
372   fact, we calculated the mean altitude at which birds were detected by the KTLX radar on each of
373   the six night in March, April, and May, and we found that the mean altitude at which birds were
374   detected on May 25, 2021 was not the highest (Table 2). It is also possible that the body size of
375   the migrants on the night of May 25 was smaller, thus making it more challenging for LunAero to
376   detect them. In fact, evidence suggests that the mean body mass of the assemblage of avian
377   migrants decreases from April to May (Horton et al., 2018). Still, it appears that on most nights,
378   LunAero can detect many of these migrants and can be used to study their movements. In fact,
379   LunAero may be able to detect low-flying migrants that may be challenging to detect using
380   weather surveillance radars (WSRs). It is also important to note that we used raw counts to
381   estimate the number of birds detected by LunAero and did not account for the fact that the
382   volume of the atmosphere sampled by LunAero is dependent on the elevational angle of the
383   moon (i.e., how close the moon is to the horizon). In fact, LunAero samples a larger volume of
384   the atmosphere, thus detecting more birds, at lower moon elevational angles (i.e., when the
385   moon is closer to the horizon) (Lowery, 1949). In the future, we will improve the ability of
386   LunAero to detect birds by accounting for the contribution of the moon elevational angle.
387   We also found a strong, statistically significant, positive correlation between the local
388   migration intensity detected by the PX-1000 radar and the regional migration intensity detected
389   by the KTLX radar on the night of May 25, 2021, preliminarily validating the ability of the PX-
390   1000 radar to detect birds (Figure 2A). The correlation between these two measures of
391   migration intensity was weak and not statistically significant across five nights in March and
392   April, but that is because the sensitivity of the PX-1000 radar was lower at close range in March
393   and April than in May (Figure 2B). As such, given its current processing pipeline, the PX-1000
394   radar could be deployed to fill the gaps left by the NEXRAD network: where there is no or low
395   spatial NEXRAD coverage or to study the movements of low-flying migrants that may be

396   challenging to detect using NEXRAD WSRs. Therefore, the PX-1000 could be used to paint a
397   more comprehensive picture of local-scale movements of migrants in conjunction with NEXRAD
398   WSRs.
399   By integrating regional migration intensity data from the KTLX radar with wind data from
400   NARR, we found evidence suggesting that birds prefer to migrate under weak wind conditions in
401   the spring (Figure 4). This finding is consistent with research that suggests that conditions with
402   low turbulence promote flight efficiency, particularly for smaller avian species (Bowlin &
403   Wikelski, 2008). Additionally, by integrating flight directional data for individual migrants from
404   LunAero with wind data from NARR, we found that when migrating under strong, southerly wind
405   conditions across six nights in March, April, and May of 2021, birds take advantage of these
406   conditions by adjusting their flight direction to match that of the wind (Figure 5A). This finding is
407   consistent with previous research showing that birds take advantage of favorable wind
408   conditions during migration (Horton et al., 2016, 2018). Our sample size is low (there were only
409   six nights for which there was LunAero data), so we cannot extrapolate these results across the
410   entirety of the spring season (or across spring seasons), but given the fact that our findings
411   match those in the literature, these analyses function as both another way to partially validate
412   the sensors in our array and to showcase the potential of multi-sensor arrays to reveal how
413   birds respond to changing wind conditions during migration.
414   We were hoping to be able to integrate avian nocturnal flight call data with data from
415   other sensors in our array; unfortunately, we were unable to collect enough nocturnal flight call
416   data to do so. We recorded the largest numbers of migrants on the nights of April 24 and May
417   25, which were also the nights with the highest regional migration intensities detected by the
418   KTLX radar, and yet, despite this fact, we only recorded 41 and 19 individuals on the nights of
419   April 24 and May 25, respectively. It is possible that the detection range of the microphone used
420   to record nocturnal flight calls is limited, as evidence suggests that detection rates of warbler
421   nocturnal flight calls are below 50% within the first 50 meters of elevation and below 25% within
422   the first 100 meters with a temperature of 20 degrees Celsius, a relative humidity of 50%, and a
423   pressure of 1013.25 hPa (Horton et al., 2015). Although the detection range of flight calls is
424   limited, they provide unique insight into species identities that are not possible to infer from
425   other data sources.
426   Our study demonstrates that multi-sensor arrays can be successfully deployed not only
427   to detect migrant birds in flight, but to understand the ways in which these birds move in
428   response to changing environmental conditions. It also sheds light on the challenges that come
429   with successfully deploying such arrays. The array we designed consisted of four different
430   sensors whose data were integrated with data from NARR, yielding five different data sources.
431   As the number of sensors and, thus, the number of data sources increases, integrating these
432   data becomes more challenging. In fact, the spatial and temporal scales of these data did not
433   always match. For example, integrating the avian nocturnal flight call data with the rest of the
434   data was challenging because we only recorded migrant flight calls on four of six nights, and
435   when we did record such calls, we recorded them infrequently over the course of those nights.
436   Mismatches in spatial and temporal scales has been recognized as a major methodological
437   challenge of data integration in macrosystems ecological research, as mismatched data need to
438   be up- or down-scaled for the extent and/or resolution to match (Rüegg et al., 2014; Zipkin et
439   al., 2021). Therefore, we recommend creating pre- and post-integration plans prior to deploying

440 multi-sensor arrays to make sure that it is possible to integrate the data in the first place and
441 that there is a contingency plan if the spatial and/or temporal scales of the data change or one
442 or more of the sensors fails.
443   Another major challenge of successfully deploying multi-sensor arrays is interdisciplinary
444 collaboration, as the collection, integration, and analysis of data from different sources requires
445 the collaboration of people from different disciplines (Rüegg et al., 2014). In our case, we
446 required knowledge in areas of study as far-ranging as radar engineering, computer vision, and
447 flight call identification. However, despite the challenges that come with successfully deploying
448 multi-sensor arrays, doing so within an interdisciplinary framework would allow us to advance
449 our understanding of avian migration at the macrosystem scale (Kelly & Horton, 2016) and
450 should be encouraged. The sample size of the data retrieved from our array was small, but that
451 is because it was meant to be a proof-of-concept array deployed within narrow spatial and
452 temporal extents; increasing the extent and resolution of the data would enhance the power of
453 such an array to detect movements of migrants over the course of a season within a region
454 across altitudes. As such arrays expand, it will become increasingly important for
455 interdisciplinary teams to adopt rigorous data management practices (Rüegg et al., 2014). As
456 we look to the future, we hope to see multi-sensor arrays being used to provide a more
457 comprehensive picture of avian migration at local, regional, and continental scales.
458
459 Conclusions
460
461 We designed a proof-of-concept multi-sensor array to study nocturnal avian spring migration in
462 central Oklahoma. This array, which consisted of a NEXRAD weather surveillance radar (WSR),
463 a portable X-band WSR, a moon-watching sensor (LunAero), and an autonomous recording unit
464 (ARU), was deployed at the University of Oklahoma Kessler Atmospheric and Ecological Field
465 Station (KAEFS) on six nights in March, April, and May of 2021. We verified that the sensors
466 agreed with one another, that is, that the intensities of avian migration recorded by most of
467 these sensors were intercorrelated. We were unable to verify that the number of individual birds
468 recorded by the ARU was consistent with the avian migration intensities detected by the other
469 sensors due to the small sample size of nocturnal avian flight calls. We also integrated data
470 from this array of sensors with wind data from the National Centers for Environmental Prediction
471 (NCEP)'s North American Regional Reanalysis (NARR) to examine the influence of this abiotic
472 variable on the movements of avian migrants aloft across these six nights in the spring. We
473 found that the number of birds detected by LunAero increased as wind velocity decreased,
474 indicating that birds prefer to migrate when winds are weak. In addition, we found that when
475 exposed to strong, southerly winds across these six nights, avian migrants took advantage of
476 these conditions by aligning their flight direction with that of the wind (i.e., drifting). Continued
477 development of the moon-watching sensor would allow us to study additional features of
478 individual migrants, such as flight velocity and body orientation, shedding light on the ways in
479 which avian migrants respond to atmospheric conditions in flight. Ultimately, expanding the
480 temporal and spatial scales at which this multi-sensor array operates holds promise for the
481 study of avian migration by providing a fuller picture of this phenomenon in time and space.
482
483 Acknowledgements

484
485 We thank the University of Oklahoma Advanced Radar Research Center engineers and
486 technicians for maintaining the PX-1000 radar and providing support during data collection. In
487 particular, Boon Leng Cheong assisted the authors with implementing scanning strategies. We
488 also thank Wesley T. Honeycutt, Angela Chen, Riley Miller, Israel Lugo, and Alyse V. Heaston
489 for their roles in the development of the LunAero hardware and analysis pipeline.
490
491 References
492

493 Aquino, C. M. S., Cheong, B., & Palmer, R. D. (2021). Progressive Pulse Compression: A Novel

494   Technique for Blind Range Recovery for Solid-State Radars. *Journal of Atmospheric and*

495   *Oceanic Technology*, *38*(9), 1599–1611. https://doi.org/10.1175/JTECH-D-20-0164.1

496 Bowlin, M. S., & Wikelski, M. (2008). Pointed Wings, Low Wingloading and Calm Air Reduce

497   Migratory Flight Costs in Songbirds. *PLOS ONE*, *3*(5), e2154.

498   https://doi.org/10.1371/journal.pone.0002154

499 Bradski, G. (2000). The OpenCV Library. *Dr. Dobb's Journal of Software Tools*.

500 Bridge, E. S., Thorup, K., Bowlin, M. S., Chilson, P. B., Diehl, R. H., Fléron, R. W., Hartl, P.,

501   Kays, R., Kelly, J. F., Robinson, W. D., & Wikelski, M. (2011). Technology on the Move:

502   Recent and Forthcoming Innovations for Tracking Migratory Birds. *BioScience*, *61*(9),

503   689–698. https://doi.org/10.1525/bio.2011.61.9.7

504 Buler, J. J., & Diehl, R. H. (2009). Quantifying Bird Density During Migratory Stopover Using

505   Weather Surveillance Radar. *IEEE Transactions on Geoscience and Remote Sensing*,

506   *47*(8), 2741–2751. https://doi.org/10.1109/TGRS.2009.2014463

507 Cheong, B. L., Kelley, R., Palmer, R. D., Zhang, Y., Yeary, M., & Yu, T.-Y. (2013). PX-1000: A

508   Solid-State Polarimetric X-Band Weather Radar and Time–Frequency Multiplexed

509   Waveform for Blind Range Mitigation. *IEEE Transactions on Instrumentation and*

510   *Measurement*, *62*(11), 3064–3072. https://doi.org/10.1109/TIM.2013.2270046

511 Chilson, P. B., Frick, W. F., Kelly, J. F., Howard, K. W., Larkin, R. P., Diehl, R. H., Westbrook, J.

512   K., Kelly, T. A., & Kunz, T. H. (2012). Partly Cloudy with a Chance of Migration: Weather,

513   Radars, and Aeroecology. *Bulletin of the American Meteorological Society*, *93*(5), 669–

514   686. https://doi.org/10.1175/BAMS-D-11-00099.1

515 Chilson, P. B., Frick, W. F., Stepanian, P. M., Shipley, J. R., Kunz, T. H., & Kelly, J. F. (2012).

516   Estimating animal densities in the aerosphere using weather radar: To Z or not to Z?

517   *Ecosphere*, *3*(8), art72. https://doi.org/10.1890/ES12-00027.1

518 Diehl, R. H., & Larkin, R. P. (2005). *Introduction to the WSR-88D (NEXRAD) for Ornithological*

519   *Research*.

520 Evans, W. R., & O'Brien, M. (2002). *Flight Calls of Migratory Birds: Eastern North American*

521   *Landbirds*. Old Bird, Inc.

522 Farnsworth, A. (2011). *A Rosetta Stone For Identifying Warblers' Migration Calls*.

523   https://www.allaboutbirds.org/news/a-rosetta-stone-for-identifying-warblers-migration-

524   calls

525 Garnier, S., & Muschelli, J. (2022). *Rvision—A computer vision library for R* (0.6.2).

526   https://swarm-lab.github.io/Rvision

527 Gauthreaux, S. A., & Belser, C. G. (1998). Displays of Bird Movements on the WSR-88D:

528   Patterns and Quantification. *Weather and Forecasting*, *13*(2), 453–464.

529   https://doi.org/10.1175/1520-0434(1998)013<0453:DOBMOT>2.0.CO;2

530 Helmus, J. J., & Collis, S. M. (2016). The Python ARM Radar Toolkit (Py-ART), a Library for

531   Working with Weather Radar Data in the Python Programming Language. *Journal of*

532   *Open Research Software*, *4*(1).

533 Hilgerloh, G., Weinbecker, J., & Zehtindjiev, P. (2006). Autumn migration of passerine

534   long-distance migrants in northern Morocco observed by moon-watching. *Ringing &*

535   *Migration*, *23*(1), 53–56. https://doi.org/10.1080/03078698.2006.9674344

536 Hill, A. P., Prince, P., Snaddon, J. L., Doncaster, C. P., & Rogers, A. (2019). AudioMoth: A low-

537   cost acoustic device for monitoring biodiversity and the environment. *HardwareX*, *6*,

538   e00073. https://doi.org/10.1016/j.ohx.2019.e00073

539   Honeycutt, W. T., & Bridge, E. S. (2022). Use of the LunAero Open-Source Hardware Platform

540   to Enhance the Accuracy and Precision of Traditional Nocturnal Migration Bird Counts.

541   *Integrative and Comparative Biology*, icac053. https://doi.org/10.1093/icb/icac053

542   Honeycutt, W. T., Heaston, A. V., Kelly, J. F., & Bridge, E. S. (2020). LunAero: Automated

543   "smart" hardware for recording video of nocturnal migration. *HardwareX*, *7*, e00106.

544   https://doi.org/10.1016/j.ohx.2020.e00106

545   Horton, K. G., Doren, B. M. V., Sorte, F. A. L., Fink, D., Sheldon, D., Farnsworth, A., & Kelly, J.

546   F. (2018). Navigating north: How body mass and winds shape avian flight behaviours

547   across a North American migratory flyway. *Ecology Letters*, *21*(7), 1055–1064.

548   https://doi.org/10.1111/ele.12971

549   Horton, K. G., Stepanian, P. M., Wainwright, C. E., & Tegeler, A. K. (2015). Influence of

550   atmospheric properties on detection of wood-warbler nocturnal flight calls. *International*

551   *Journal of Biometeorology*, *59*(10), 1385–1394. https://doi.org/10.1007/s00484-014-

552   0948-8

553   Horton, K. G., Van Doren, B. M., Stepanian, P. M., Hochachka, W. M., Farnsworth, A., & Kelly,

554   J. F. (2016). Nocturnally migrating songbirds drift when they can and compensate when

555   they must. *Scientific Reports*, *6*(1), Article 1. https://doi.org/10.1038/srep21249

556   K. Lisa Yang Center for Conservation Bioacoustics at the Cornell Lab of Ornithology. (2022).

557   *Raven Pro: Interactive Sound Analysis Software* (1.6.3). Cornell Lab of Ornithology.

558   https://ravensoundsoftware.com

559   Kelly, J. F., & Horton, K. G. (2016). Toward a predictive macrosystems framework for migration

560   ecology. *Global Ecology and Biogeography*, *25*(10), 1159–1165.

561   https://doi.org/10.1111/geb.12473

562   Kilambi, A., Fabry, F., & Meunier, V. (2018). A Simple and Effective Method for Separating

563   Meteorological from Nonmeteorological Targets Using Dual-Polarization Data. *Journal of*

564   *Atmospheric and Oceanic Technology*, *35*(7), 1415–1424.

565   https://doi.org/10.1175/JTECH-D-17-0175.1

566 Kurdzo, J. M., Cheong, B. L., Palmer, R. D., Zhang, G., & Meier, J. B. (2014). A Pulse

567   Compression Waveform for Improved-Sensitivity Weather Radar Observations. *Journal*

568   *of Atmospheric and Oceanic Technology*, *31*(12), 2713–2731.

569   https://doi.org/10.1175/JTECH-D-13-00021.1

570 Landsborough, B. J., Foote, J. R., & Mennill, D. J. (2019). Decoding the 'zeep' complex:

571   Quantitative analysis of interspecific variation in the nocturnal flight calls of nine wood

572   warbler species (Parulidae spp.). *Bioacoustics*, *28*(6), 555–574.

573   https://doi.org/10.1080/09524622.2018.1509373

574 Larkin, R. P., Evans, W. R., & Diehl, R. H. (2002). Nocturnal Flight Calls of Dickcissels and

575   Doppler Radar Echoes over South Texas in Spring (Llamadas durante vuelos nocturnos

576   sobre Texas de Spiza americana durante la primavera y el eco en un radar Doppler).

577   *Journal of Field Ornithology*, *73*(1), 2–8.

578 Liechti, F., Aschwanden, J., Blew, J., Boos, M., Brabant, R., Dokter, A. M., Kosarev, V., Lukach,

579   M., Maruri, M., Reyniers, M., Schekler, I., Schmaljohann, H., Schmid, B., Weisshaupt,

580   N., & Sapir, N. (2019). Cross-calibration of different radar systems for monitoring

581   nocturnal bird migration across Europe and the Near East. *Ecography*, *42*(5), 887–898.

582   https://doi.org/10.1111/ecog.04041

583 Liechti, F., Bruderer, B., & Paproth, H. (1995). Quantification of Nocturnal Bird Migration by

584   Moonwatching: Comparison with Radar and Infrared Observations (Cuantificación de la

585   Migración Nocturna de Aves Observando la Luna: Comparación con Observaciones de

586   Radar e Intrarrojas). *Journal of Field Ornithology*, *66*(4), 457–468.

587 Lowery, G. H. (1949). *A quantitative study of the nocturnal migration of birds*.

588   https://kuscholarworks.ku.edu/handle/1808/26277

589   Lowery, G. H., Jr., & Newman, R. J. (1966). A Continentwide View of Bird Migration on Four

590   Nights in October. *The Auk*, *83*(4), 547–586. https://doi.org/10.2307/4083149

591   McKinnon, E. A., & Love, O. P. (2018). Ten years tracking the migrations of small landbirds:

592   Lessons learned in the golden age of bio-logging. *The Auk*, *135*(4), 834–856.

593   https://doi.org/10.1642/AUK-17-202.1

594   Nilsson, C., Dokter, A. M., Schmid, B., Scacco, M., Verlinden, L., Bäckman, J., Haase, G.,

595   Dell'Omo, G., Chapman, J. W., Leijnse, H., & Liechti, F. (2018). Field validation of radar

596   systems for monitoring bird migration. *Journal of Applied Ecology*, *55*(6), 2552–2564.

597   https://doi.org/10.1111/1365-2664.13174

598   Nisbet, I. C. T. (1959). Calculation of Flight Directions of Birds Observed Crossing the Face of

599   the Moon. *The Wilson Bulletin*, *71*(3), 237–243.

600   Robinson, W. D., Bowlin, M. S., Bisson, I., Shamoun-Baranes, J., Thorup, K., Diehl, R. H.,

601   Kunz, T. H., Mabey, S., & Winkler, D. W. (2010). Integrating concepts and technologies

602   to advance the study of bird migration. *Frontiers in Ecology and the Environment*, *8*(7),

603   354–361. https://doi.org/10.1890/080179

604   Rüegg, J., Gries, C., Bond-Lamberty, B., Bowen, G. J., Felzer, B. S., McIntyre, N. E., Soranno,

605   P. A., Vanderbilt, K. L., & Weathers, K. C. (2014). Completing the data life cycle: Using

606   information management in macrosystems ecology research. *Frontiers in Ecology and*

607   *the Environment*, *12*(1), 24–30. https://doi.org/10.1890/120375

608   Trösch, B., Lardelli, R., Liechti, F., Peter, D., & Bruderer, B. (2005). Spatial and seasonal

609   variation in nocturnal autumn and spring migration patterns in the western

610   Mediterranean area: A moon-watching survey. *Avocetta*, *29*, 63–73.

611   Wainwright, C. E., Stepanian, P. M., & Horton, K. G. (2016). The role of the US Great Plains

612   low-level jet in nocturnal migrant behavior. *International Journal of Biometeorology*,

613   *60*(10), 1531–1542. https://doi.org/10.1007/s00484-016-1144-9

614   Weisshaupt, N., Lehmann, V., Arizaga, J., & Maruri, M. (2017). Radar wind profilers and avian

615   migration: A qualitative and quantitative assessment verified by thermal imaging and

616   moon watching. *Methods in Ecology and Evolution*, *8*(9), 1133–1145.

617   https://doi.org/10.1111/2041-210X.12763

618   Weisshaupt, N., Lehtiniemi, T., & Koistinen, J. (2021). Combining citizen science and weather

619   radar data to study large-scale bird movements. *Ibis*, *163*(2), 728–736.

620   https://doi.org/10.1111/ibi.12906

621   Weisshaupt, N., Maruri, M., & Arizaga, J. (2016). Preliminary assessment of nocturnal bird

622   migration at the Bay of Biscay as observed by moon-watching. *Munibe*, *64*.

623   https://doi.org/10.21630/mcn.2016.64.03

624   Zehtindjiev, P., & Liechti, F. (2003). A quantitative estimate of the spatial and temporal

625   distribution of nocturnal bird migration in south-eastern Europe -a coordinated moon-

626   watching study. *Avian Science*, *3*.

627   Zipkin, E. F., Zylstra, E. R., Wright, A. D., Saunders, S. P., Finley, A. O., Dietze, M. C., Itter, M.

628   S., & Tingley, M. W. (2021). Addressing data integration challenges to link ecological

629   processes across scales. *Frontiers in Ecology and the Environment*, *19*(1), 30–38.

630   https://doi.org/10.1002/fee.2290

631   Zotti, G., Hoffmann, S. M., Wolf, A., Chéreau, F., & Chéreau, G. (2021). *The Simulated Sky:*

632   *Stellarium for Cultural Astronomy Research. Journal of Skyscape Archaeology*.

633

Figure 1

Relationship between the number of birds detected by LunAero and the regional avian migration intensity from KTLX in the atmosphere above KAEFS on select nights in March, April, and May of 2021.

Each data point corresponds to a one-hour period on the night of March 26, March 27, March 28, March 29, April 24, or May 25, 2021. Each date is associated with a different color.
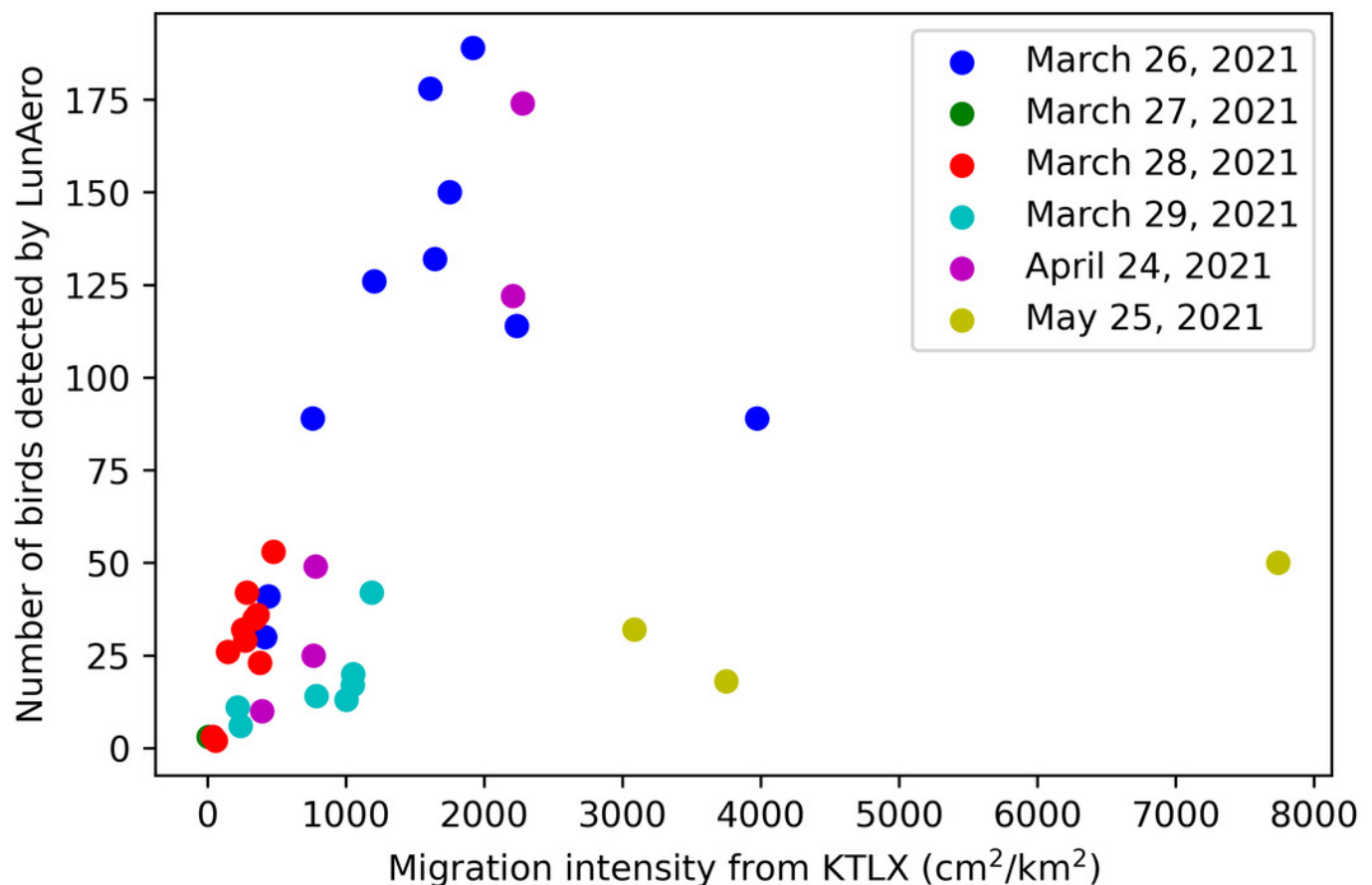
Figure 2

Relationship between the local avian migration intensity detected by PX-1000 and the regional avian migration intensity detected by KTLX in the atmosphere above KAEFS in the spring of 2021.

(A) Relationship on the night of May 25, 2021. (B) Relationship on the nights of March 26, March 27, March 28, March 29, and April 24, 2021. Each data point corresponds to a ~ten-minute period, which is the temporal resolution of the KTLX weather surveillance radar (WSR).

(A) Migration intensities from PX-1000 and KTLX on the night of May 25, 2021
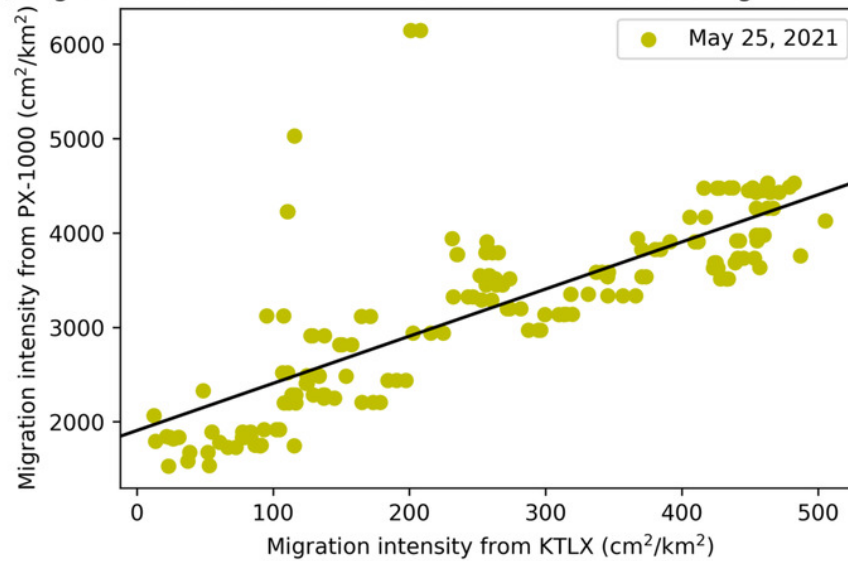
(B) Migration intensities from PX-1000 and KTLX on select nights in March and April of 2021
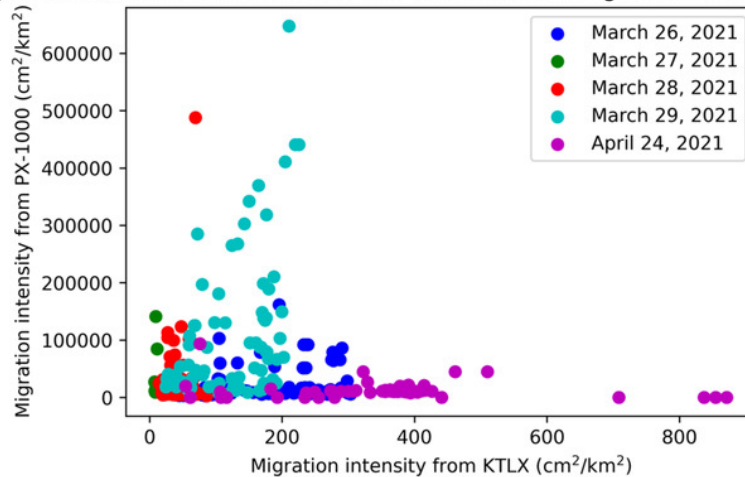
Figure 3

Direction and velocity of the wind in the atmosphere above the Kessler Atmospheric and Ecological Field Station (KAEFS) on select nights in March, April, and May of 2021.

This polar plot shows wind direction as the angle in degrees clockwise from north and velocity as the distance between the data point and the origin. Each data point corresponds to a three-hour period for a given date, represented by a color. This data stems from the National Centers for Environmental Prediction (NCEP)'s North American Regional Reanalysis (NARR).
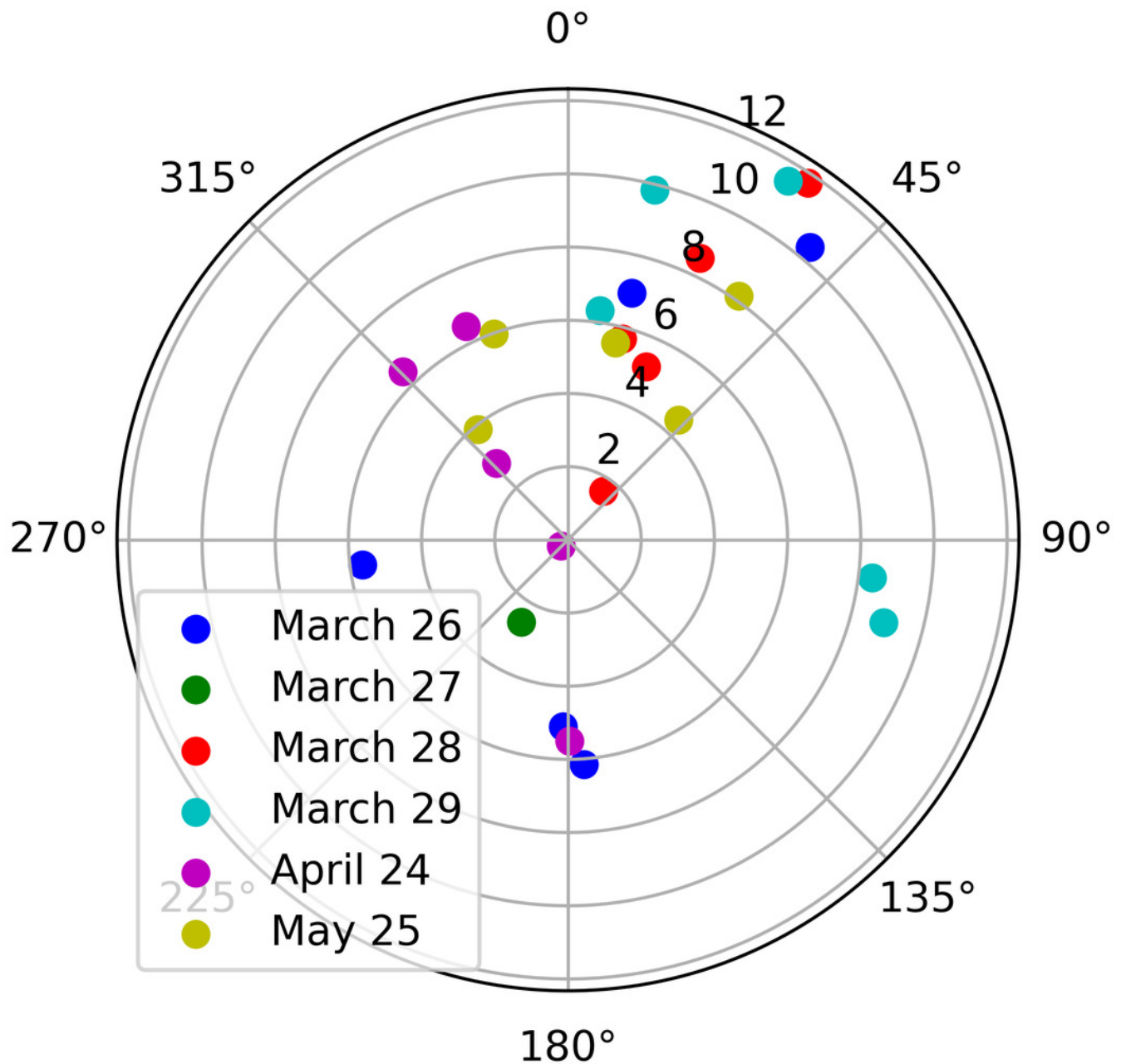
Figure 4

Relationship between regional avian migration intensity detected by KTLX and wind velocity in the atmosphere above KAEFS on select nights in March, April, and May of 2021.

Each data point corresponds to a ~ten-minute period, which is the temporal resolution of the KTLX weather surveillance radar (WSR), for the nights of March 26, March 27, March 28, March 29, April 24, and May 25 of 2021. The wind data stems from the NCEP's NARR.
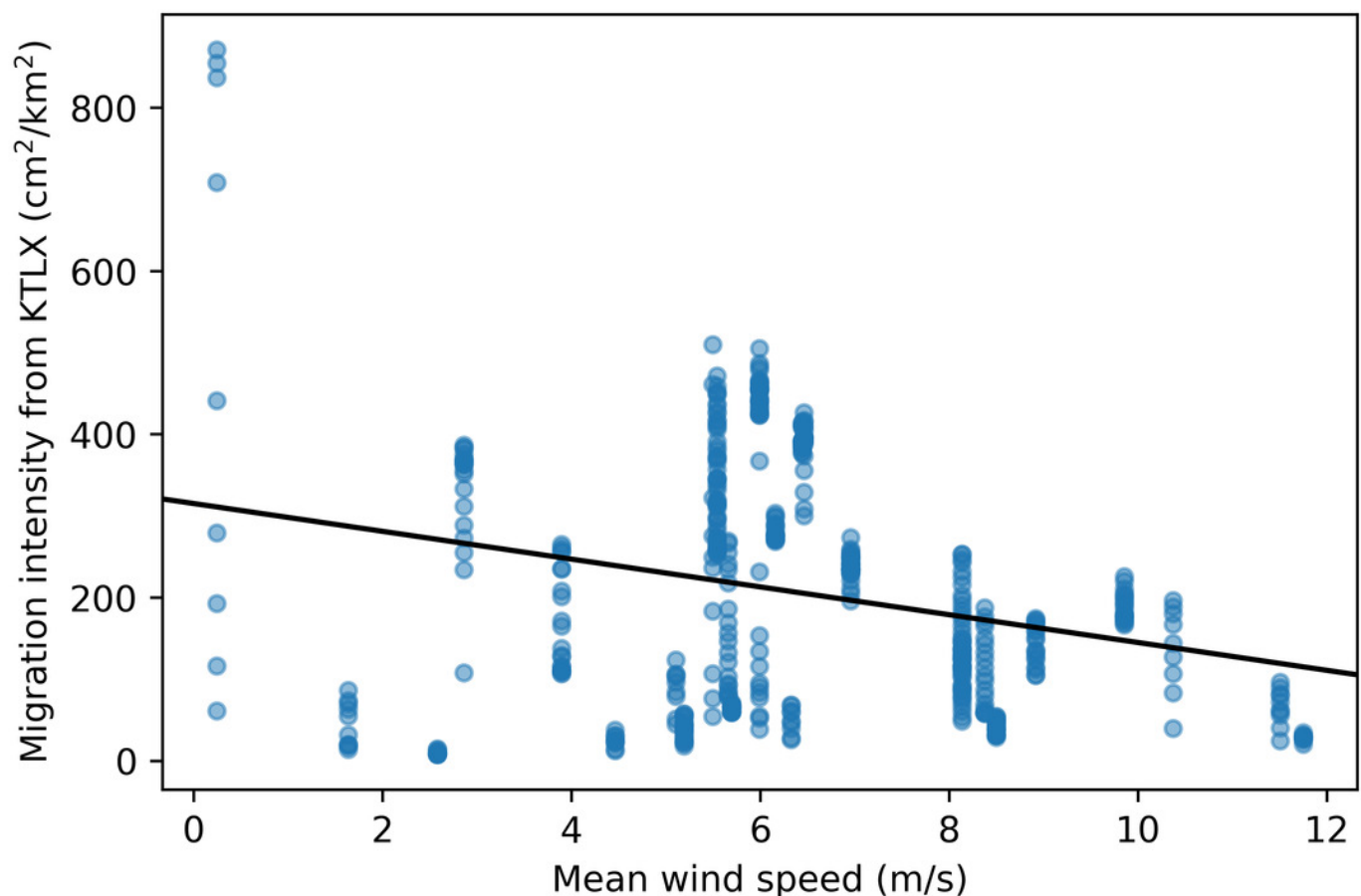
Figure 5

Difference between the flight direction of individual birds detected by LunAero and the direction of the wind as a function of wind velocity in the atmosphere above KAEFS in the spring of 2021.

(A) Southerly and (B) northerly winds. Southerly winds are winds with direction angles between 90 and 270 degrees clockwise from north, while northerly winds are winds with direction angles between 270 and 0 degrees and between 0 and 90 degrees clockwise from north. The black dots represent mean differences for discrete wind velocity values. The data correspond to the nights of March 26, March 27, March 28, March 29, April 24, and May 25, 2021. The wind data stems from the NCEP's NARR.
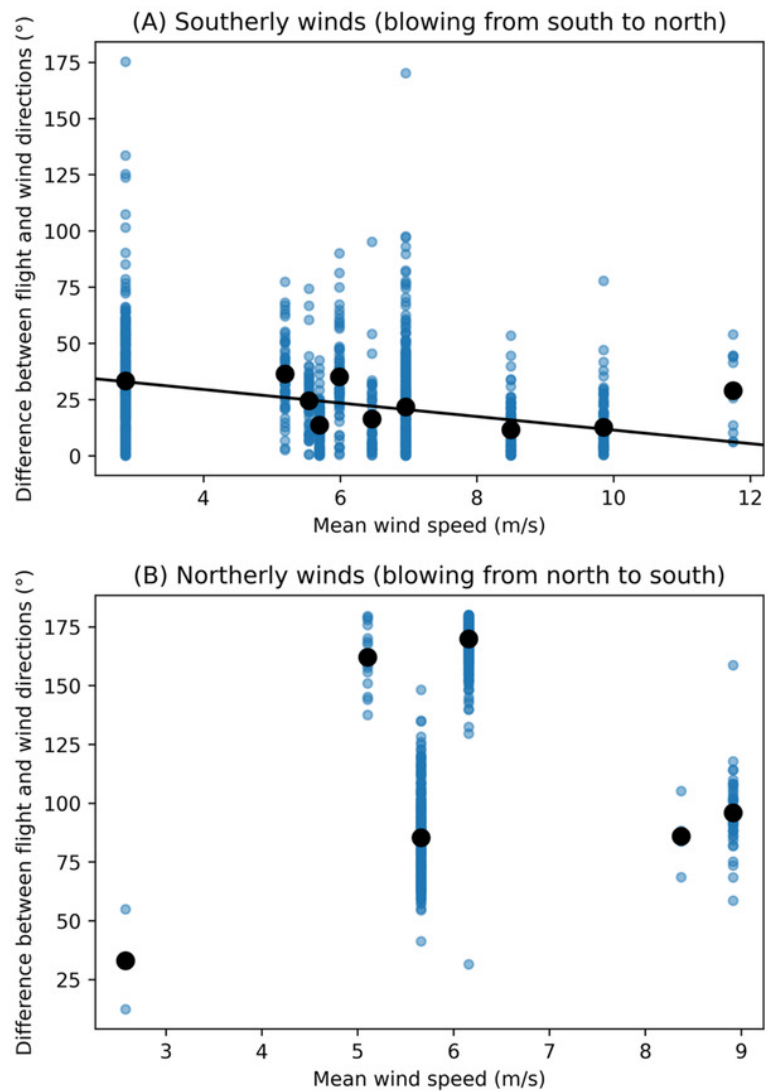
Avian species and number of individuals detected via nocturnal avian flight calls in the atmosphere above KAEFS on select nights in March, April, and May of 2021.

Nocturnal avian flight calls were recorded by an autonomous recording unit (ARU) on the nights of March 27, March 29, April 24, and May 25, 2021. Higher-intensity colors indicate larger numbers of individuals detected, with the exception of the grand total, which was not highlighted.

	Scientific name	Common name	March 27, 2021	March 29, 2021	April 24, 2021	May 25, 2021	Number of individuals per species
	Protonotaria citrea	Prothonotary Warbler	1	0	0	0	1
	Passerculus sandwichensis	Savannah Sparrow	3	0	4	0	7
	Branta canadensis	Canada Goose	0	1	0	0	1
	Calidris melanotos	Pectoral Sandpiper	0	1	0	0	1
	Spizella pallida	Clay-colored Sparrow	0	0	4	0	4
	Spizella passerina	Chipping Sparrow	0	0	1	1	2
	Ammodramus savannarum	Grasshopper Sparrow	0	0	5	0	5
	Tringa flavipes	Lesser Yellowlegs	0	0	1	0	1
	Catharus ustulatus	Swainson's Thrush	0	0	4	17	21
	Bartramia longicauda	Upland Sandpiper	0	0	14	0	14
	Pooecetes gramineus	Vesper Sparrow	0	0	2	0	2
	Zonotrichia leucophrys	White-crowned Sparrow	0	0	3	0	3
	Cardellina pusilla	Wilson's Warbler	0	0	2	0	2
	Zonotrichia albicollis	White-throated Sparrow	0	0	1	0	1
	Setophaga petechia	Yellow Warbler	0	0	0	1	1
Number of individuals per day			4	2	41	19	66

Mean altitude at which birds were detected by the KTLX radar on six nights in March, April, and May of 2021.

Mean altitude at which birds were detected by the KTLX radar on six nights in March, April, and May of 2021.

Date	Mean altitude above mean sea level (meters)
March 26, 2021	770.210404
March 27, 2021	537.570479
March 28, 2021	667.877065
March 29, 2021	749.929377
April 24, 2021	689.156399
March 25, 2021	733.208123